Exact steady-state velocity of ratchets driven by random sequential adsorption

Maria R D'Orsogna[1], **Tom Chou**[1,2] **and Tibor Antal**[3]

[1] Department of Mathematics, UCLA, Los Angeles, CA 90095-1555, USA
[2] Department of Biomathematics, UCLA, Los Angeles, CA 90095-1766, USA
[3] Program for Evolutionary Dynamics, Harvard University, Cambridge,
MA 02138, USA

Abstract

We solve the problem of discrete translocation of a polymer through a pore, driven by the irreversible, random sequential adsorption of particles on one side of the pore. Although the kinetics of the wall motion and the deposition are coupled, we find the exact steady-state distribution for the gap between the wall and the nearest deposited particle. This result enables us to construct the mean translocation velocity demonstrating that translocation is faster when the adsorbing particles are smaller. Monte Carlo simulations also show that smaller particles give less dispersion in the ratcheted motion. We also define and compare the relative efficiencies of ratcheting by deposition of particles with different sizes and we describe an associated 'zone-refinement' process.

Introduction

Polymer translocation through membrane nanopores is a common process in living cells. The transport of proteins and nucleic acids, in and out of organelles, serves a variety of control, signalling and error correction functions [1–3]. Recent advances in polymer manipulation at the nanoscale level have also sparked interest in pore translocation as a new tool in genetic sequencing, structure determination and drug delivery [4–6]. Active polymer transport through pores requires driving forces which are often provided by 'chaperone' proteins that bind to the polymer on one side of the membrane. The proteins are larger than the pore and, once bound, create a barrier blocking backward polymer fluctuations. This ratcheting process eventually drives the entire polymer through the pore. Another known translocation mechanism is by 'power-stroke' [3, 7], where chaperones that are deposited close to the membrane are subject to conformational changes. These induce a strain that is relieved only by direct pulling of the protein through the pore, similar to the driving mechanisms of motors such as myosin and kinesin [8]. In post-translational protein translocation, both Brownian ratcheting [9, 10] and
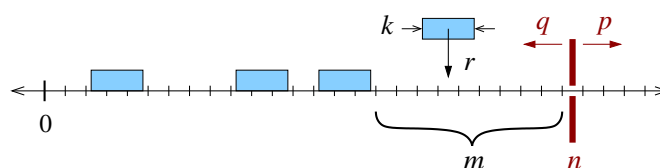
Figure 1. Random sequential adsorption of chaperone particles of k lattice sites, with the deposition rate r. In the polymer reference frame, the fluctuating wall has intrinsic hopping rates p, q and is ratcheted by the irreversibly bound particles. In the case of Hsp70 proteins binding to nucleic acids, $k \sim 6$.

power stroke [11] pulling, mediated by Hsp-70 ATPases, have been proposed. Both models exhibit qualitatively similar behaviour and cannot be distinguished by experimental data [3]. However, translocation by power stroke is molecularly more complex, its modelling requires additional parameters [3, 12] and its effects arise only at extremely high binding protein densities [7]. Thus, we will only consider Brownian ratcheting as the dominant translocation driving force, and neglect power stroke mechanisms.

Solution of random sequential adsorption ratchet

The problem of translocating polymers driven by Brownian ratchets has been considered by many authors. Analytical progress, however, has been possible only for certain limiting cases where restrictions are placed on the binding kinetics. For instance, continuum Fokker–Planck models have been solved [1–3, 7] only in the limit of perfect ratchets where particles are forced to deposit next to the membrane, or in the limit of rapid particle equilibration (Langmuir kinetics). While the continuum approach is justifiable in the limit of large chaperone particles that occupy $k \gg 1$ lattice sites, in many applications this limit may be unrealistic. For instance, chaperones of the Hsp70 family, commonly employed in polymer translocation across the endoplasmic reticulum, are approximately 2 nm in size. If we assume polymers of nucleic acids with interbase distances of $\sim$0.36 nm, and that the polymer diffuses one base pair at a time, typical Hsp70 class chaperones would be described by binding particles with $k \sim 6$. For the translocation of such structures, the discrete approach is more pertinent. Random chaperone particle deposition was recently studied using a discrete master equation, and including particle detachment and diffusion. However, results were derived only in the limit of rapid equilibration, either of the binding particles or of the fluctuating polymer [13]. In this paper, we report an exact steady-state solution of the discrete translocation process in the irreversible deposition limit. In our model, the only constraint is that the binding particles do not overlap. No other approximations are made. As in the previous work we will only consider stiff polymers that do not contribute conformational entropy [2, 7, 13]. The dependence of the mean velocity on the size of the deposited particles is explicitly computed. Our result for the mean translocation velocity is verified using Monte Carlo simulations. Simulation results for the dispersion of the translocation are also discussed.

Consider particles of integer length k irreversibly binding to an infinitely long one-dimensional lattice representing the translocating polymer. The fluctuating polymer is assumed to jump one unit to the right or left with rates q and p, respectively. In the reference frame of the polymer, as shown in figure 1, the membrane wall hops forward and backward with rates p and q, respectively. Particle deposition occurs at rate r only if there are at least k open sites between the wall and the nearest deposited particle. The dynamics of the wall is closely related to that of its nearest gap, since wall fluctuations are allowed only if there are enough

empty sites for the wall to perform its random motion. Ratcheting occurs when a gap is large enough for a particle to irreversibly deposit, preventing the wall from sliding backwards. After deposition, particles cannot diffuse nor detach.

The master equation for the probability density $P_{m,n}(t)$ for a wall to be at position $n \in (-\infty, \infty)$ and for the gap closest to it to be of length $m \in [0, \infty)$ can be derived in analogy with problems in random sequential adsorption (RSA) [14, 15]. While in RSA all gaps are equivalent and one is concerned with the probability of finding a gap of length m anywhere along the infinite lattice, here we are interested in the random deposition of particles in the *single* gap between the wall and its nearest particle, as shown in figure 1. The time evolution of $P_{m,n}(t)$ obeys

$$\dot{P}_{m,n} = pP_{m-1,n-1} + qP_{m+1,n+1} - [p + q + r(m - k + 1)H_{m-k}]P_{m,n} + r\sum_{j=m+k}^{\infty} P_{j,n}, \tag{1}$$

where the Heaviside function $H_{m-k} = 1$ for $m \geqslant k$ and zero otherwise. For $m = 0$, $\dot{P}_{0,n}(t) = qP_{1,n+1} - pP_{0,n} + r\sum_{j=k}^{\infty} P_{j,n}$. The terms with p, q represent the hopping of a free, non-interacting wall, which by themselves would lead to a wall drift proportional to $p - q$. The other terms in equation (1) describe RSA dynamics. A gap of length m can be produced by the deposition of a k-mer in a gap of arbitrary length $j \geqslant m + k$. Although there are $j - k + 1$ ways, each with rate r, of depositing a k-mer in such a gap, only one of these choices will lead to the creation of a gap of length m. Similarly, a gap of length m can be destroyed by the deposition of any particle of length k within it, a process which occurs in $(m - k + 1)$ ways for an overall destruction rate of $r(m - k + 1)$. For $m < k$, no deposition-mediated gap destruction occurs because a k-mer cannot fit into such a small gap. On summing $P_{m,n}(t)$ over all values $m \in [0, \infty)$ to define $Q_n(t) \equiv \sum_m P_{n,m}(t)$, the terms pertaining to the RSA process cancel exactly and

$$\dot{Q}_n = p[Q_{n-1} - Q_n] + q[Q'_{n+1} - qQ'_n], \tag{2}$$

where $Q'_n \equiv Q_n - P_{0,n}$ is the conditional probability that the wall is at position n and that the site preceding it is empty. On multiplying equation (2) by n and summing over the infinite lattice,

$$\frac{d\langle n(t)\rangle}{dt} = p - q\sum_{j=-\infty}^{\infty} Q'_j \equiv p - q\langle \sigma \rangle, \tag{3}$$

where $\langle \sigma \rangle \equiv \sum_{j=-\infty}^{\infty} Q'_j$ is the probability that the site immediately preceding the wall is empty. This definition implies that $\langle \sigma \rangle$, the realization-averaged value of the random vacancy variable σ in the frame of the wall, is also the probability for a gap of nonzero length to exist between the wall and the nearest particle. Provided Q'_j reaches its steady-state distribution in finite time, equation (3) defines the steady-state mean wall velocity

$$v = p - q\langle \sigma \rangle. \tag{4}$$

Note that the dependence of the average velocity v on the deposition rate r resides completely in the term $\langle \sigma \rangle$. What remains is to find an explicit steady-state expression for $\langle \sigma \rangle = \sum_j Q'_j$. To this end, we sum equation (1), this time over both wall positions $n \in (-\infty, \infty)$ and over gap lengths $m' \geqslant m$ obtaining the cumulative probability distribution for the first gap to be of length m or larger $R_m \equiv \sum_{m'=m}^{\infty} \sum_{n=-\infty}^{\infty} P_{m,n}(t \to \infty)$. We may now recognize that $R_1 = \langle \sigma \rangle$, since the probability for a gap of nonzero length to exist adjacent to the wall is equivalent to the probability that the gap is of *any* length except zero. Thus, in order to find exact expressions for the velocity in equation (4) we need to find R_1. Performing the

sums over n and m' in the steady-state limit of equation (1), we obtain the recursion relation for R_m,

$$[p + q + r(m - k + 1)H_{m-k+1}] R_m = q R_{m+1} + p R_{m-1} - r \sum_{j=\max\{k,m+1\}}^{m+k-1} R_j, \qquad (5)$$

along with the normalization condition $R_0 = 1$. Equation (5) is solved by introducing the z-transform,

$$G(z) \equiv \sum_{m=-\infty}^{\infty} z^m R_m, \qquad (6)$$

and its inverse

$$R_m = \oint_C \frac{G(z)}{z^{m+1}} \frac{\mathrm{d}z}{2\pi\mathrm{i}}, \qquad (7)$$

given by the Cauchy integral encircling the origin [16]. Although physically $m \in [0, \infty)$, the z-transform is a sum over all integers, extending the definition to $R_{m<0}$. In order to z-transform equation (5) we set H_{m-k+1} to unity regardless of m. In this case, we find a first-order differential equation for $G(z)$ which is solved by

$$G(z) = \frac{G_0 z^k}{z^{p+q+1}} \exp\left(pz - \frac{q - H_{k-2}}{z} + \sum_{j=3}^{k} \frac{z^{1-j}}{j-1} \right). \qquad (8)$$

For notational simplicity, equations (8)–(13) are expressed with the rates p and q normalized by the deposition rate r. The R_m arising from inverting equation (8) are valid only for $m \geqslant k - 2$ since the smallest m for which $H_{m-k+1} = 1$ is $m = k - 1$ and since, for $m = k - 1$, equation (5) contains R_{k-2}. For $k = 1, 2$, the last term in the exponent of equation (8) vanishes and the above generating function is valid for all values of m. The Cauchy integral formula thus yields R_m for all values of $m > 0$. The integration constant G_0 can be fixed by directly applying the condition $R_0 = 1$. For $k = 1$ we find

$$R_m = \left(\frac{p}{q} \right)^{m/2} \frac{J_{p+q+m}(2\sqrt{pq})}{J_{p+q}(2\sqrt{pq})}, \qquad k = 1, \qquad (9)$$

where J_ν is the Bessel function of the first kind of order ν. For dimers, $G(z)$ is identical to the $k = 1$ case except for the substitution $q \to q - 1$ in equation (8). For $q > 1$, the form of R_m is the same as in equation (9), with the same substitution in q. If we define $Z_\nu \equiv J_\nu$ for $q > 1$ and $Z_\nu \equiv I_\nu$ for $q < 1$, where I_ν is the modified Bessel function of order ν, for $k = 2$ we obtain

$$R_m = \frac{p^{m/2}}{|q-1|^{m/2}} \frac{Z_{p+q+m-1}(2\sqrt{p|q-1|})}{Z_{p+q-1}(2\sqrt{p|q-1|})}, \qquad k = 2. \qquad (10)$$

For $q = 1$ in the $k = 2$ case, the direct inverse z-transform gives $R_m = p^m \Gamma(p+1)/\Gamma(p+m+1)$, where Γ is the Gamma function.

Next, consider the case of larger particles $k \geqslant 3$. The $R_{m \geqslant k-2}$ arising from equation (8) must now be coupled with explicit solutions for $R_{m \leqslant k-3}$ from equation (5), where $H_{m-k+1} = 0$. Let us derive $R_{m \geqslant k-2}$ from the generating function $G(z)$. If we define $a_j^{(k)}$ as the jth term in the Laurent series appearing in equation (8), $\exp\left(\sum_{j=2}^{k-1} z^{-j}/j \right) \equiv \sum_{j=0}^{\infty} a_j^{(k)} z^{-j}$, we can write R_m for $m \geqslant k - 2$ as

$$R_m = G_0 \sum_{j=0}^{\infty} \frac{a_j^{(k)} p^{\alpha/2}}{|q-1|^{\alpha/2}} Z_\alpha(2\sqrt{p|q-1|}), \qquad k \geqslant 3, \qquad (11)$$
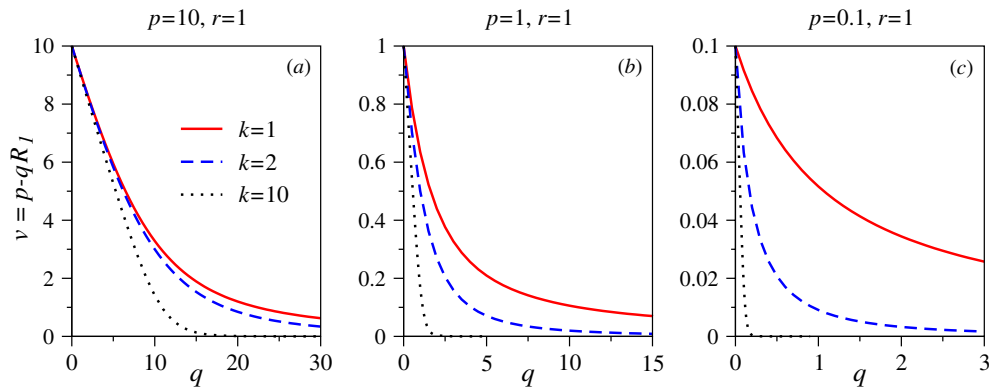
Figure 2. (a)–(c) Exact steady-state velocities as functions of q for $r = 1$, $p = 0.1, 1, 10$ at different particle sizes $k = 1, 2, 10$. Departure from a simple biased random walk occurs for large q/p. The irreversible deposition of particles ensures $v > 0$. For each set of values p, q, the maximal velocity arises for the smallest possible particles, when $k = 1$.

where $\alpha \equiv j + p + q - k + 1 + m$. These z-transformed solutions are valid only for $m \geqslant k - 2$, for which we let $R_m \equiv G_0 \tilde{R}_m$. In order to apply the condition $R_0 = 1$ and determine G_0, we must connect equation (11) to the $m \leqslant k - 2$ equations in (5). These involve R_m up to $m = 2k - 3$. G_0 can thus be determined by

$$
\mathbf{M} \cdot \begin{pmatrix} R_1 \\ \vdots \\ R_{k-3} \\ G_0 \tilde{R}_{k-2} \\ \vdots \\ G_0 \tilde{R}_{2k-3} \end{pmatrix} = - \begin{pmatrix} p \\ \vdots \\ 0 \\ 0 \\ \vdots \\ 0 \end{pmatrix},
\tag{12}
$$

where $\mathbf{M}$ is the $(2k - 3) \times (k - 2)$ transition matrix describing the linear subsystem in equation (5):

$$
\mathbf{M} = \begin{pmatrix} -(p+q) & q & 0 & \dots & 0 & -1 & 0 & 0 & \cdots \\ p & -(p+q) & q & \dots & 0 & -1 & -1 & 0 & \cdots \\ 0 & p & -(p+q) & \dots & 0 & -1 & -1 & -1 & \cdots \\ \vdots & \vdots & \vdots & \dots & \vdots & \vdots & \vdots & \vdots & \vdots \\ 0 & \cdots & 0 & \dots & q & -1 & -1 & \cdots & -1 \end{pmatrix}.
\tag{13}
$$

Solving equation (12) allows us to determine G_0 and the exact gap distribution R_m for all parameters p, q, r, k.

Velocity and dispersion

In figures 2(a)–(c), we plot the average wall velocity $v = p - q R_1$ as functions of the backward hopping rate q, for various particle lengths k and forward hopping rates p. Ratcheting from particle deposition is stronger when q/p is large, the wall motion is biased towards the deposited particles, and R_1 is small. For fixed kinetic parameters, particles of smaller size k yield faster translocation and smaller variance. Smaller particles are more effective at translocation due to their enhanced insertion rate into the fluctuating gap despite taking

smaller steps than larger particles. The relative difference of the velocity and dispersion among different particle sizes is most pronounced in the strongly ratcheting regime where q/p is large.

Now consider the dispersion of the ratcheted wall. On multiplying equation (2) by n^2 and summing over all integers n, we find

$$\frac{\mathrm{d}}{\mathrm{d}t} \langle n^2 \rangle = p + q \langle \sigma \rangle + 2p \langle n \rangle - 2q \sum_{n=-\infty}^{\infty} n Q_n'. \tag{14}$$

For this calculation, we cannot simply use $\langle n \rangle = vt$ as implied by equation (4). Although one expects the realization-averaged $\langle \sigma \rangle$ to exponentially decay to its steady-state value, an initial transient exists before the distributions reach steady state. Incorporating an 'integration constant' arising from this transient, and integrating equation (3) (with $n(0) = 0$), we define

$$\langle n(t) \rangle = pt - q \int_0^t \langle \sigma \rangle \, \mathrm{d}t \equiv vt + n_0. \tag{15}$$

Similarly, we define

$$\langle n' \rangle \equiv \frac{\sum_{n=-\infty}^{\infty} n Q_n'}{\sum_{n=-\infty}^{\infty} Q_n'} \equiv \frac{\sum_{n=-\infty}^{\infty} n Q_n'}{\langle \sigma \rangle} = vt + n_0'. \tag{16}$$

The two *different* integration constants n_0 and n_0' that embody the initial transients do not affect the determination of the steady-state velocity $v = \mathrm{d}\langle n(t) \rangle / \mathrm{d}t$, but interestingly, affect the wall dispersion. On computing $\langle n^2 \rangle - \langle n \rangle^2 = 2Dt$, we find

$$2D = p + q \langle \sigma \rangle [1 - 2(n_0' - n_0)]. \tag{17}$$

The dispersion D retains memory of the transients during which the averaged velocities have not yet reached v. This contribution to the dispersion is embodied in the $n_0' - n_0$ term in equation (17). The term $n_0' - n_0$ is always positive because it takes longer for a wall with a gap to reach terminal velocity than an unrestricted wall, leading to a larger intercept n_0'. Therefore, $p + q \langle \sigma \rangle$ is an upper bound for $2D$ that is accurate for $k = 1$ in the $r \to \infty$ limit where $\langle \sigma \rangle \to 0$.

In figure 3, we show both the mean velocity v and dispersion D of the wall, this time as functions of r, with fixed $p = q = 1$. As r is increased, not only does the mean velocity v increase but so does the dispersion D. Although the wall is 'pushed' harder by the rapidly deposited particles, its typical displacement also increases to slightly overcompensate the sharpening effect of imposing reflecting boundary conditions at each deposited particle. In the $r \to 0$ limit, we expect the dispersion to approach that of a diffusing particle with reflecting boundary conditions on one side: $D = p(1 - 2/\pi) \approx 0.3634p$ for $q = p$. The Monte Carlo value for $p = q = k = 1$ and $r = 10^{-3}$ gives $D = 0.388$ in good agreement with the expected result.

Our results can also be simplified in the limit of infinitely fast particle deposition, where a particle is deposited as soon as the first gap reaches a length of k lattice sites. The dynamics then becomes that of the so-called burnt-bridge model [17–20]. In the one-dimensional burnt-bridge model, certain links (bridges) separated by k lattice sites can be crossed only once by the walk, which then generates a biased motion. The speed and the diffusion coefficient can be calculated by either using the continuous time version of the discrete time method in [19] or
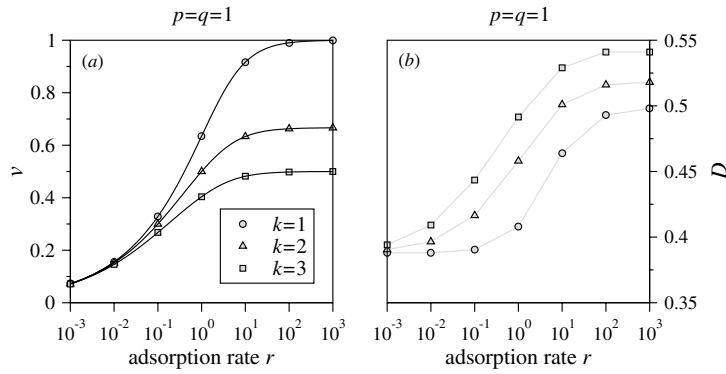
Figure 3. Velocities and dispersions as a function of the deposition rate r for fixed $p = q = 1$ and $k = 1, 2, 3$. (*a*) The mean velocity v for $k = 1, 2, 3$. Both Monte Carlo results and the exact solution are shown together. (*b*) Monte Carlo results for the dispersion D. For $r \gg p, q$, the limiting values (from equation (19) for D are $1/2$, $14/27$ and $13/24$ for $k = 1, 2$ and 3, respectively.

by using the general results in [21], as has been done in [20] for an unbiased ($p = q$) random walk. For $r \gg p, q$, we obtain

$$
\begin{aligned}
v &= \frac{pk(a-1)^2}{a(a^k - 1) + k(1 - a)} \\
D &= \frac{pk^2(a-1)^2[a^{2k+2} + 4a^{k+1}(k + 1 - ka) + k(1 - a^2) - a(a + 4)]}{2[a(a^k - 1) + k(1 - a)]^3}
\end{aligned}
\tag{18}
$$

where $a \equiv q/p$. These expressions simplify further in the symmetric case $p = q$:

$$
v = \frac{2p}{k+1} \qquad D = \frac{2}{3} \frac{k^2 + k + 1}{(k+1)^2} p.
\tag{19}
$$

In the large k limit, appropriate for large binding proteins such as single-stranded binding proteins (SSB) with $k \approx 60$, the average velocity and dispersion also take on simple limiting forms. For $a = q/p > 1$, the large k limits of v and D given in equation (18) are

$$
v = \frac{pk(a-1)^2}{a^{k+1}}, \qquad D = \frac{pk^2(a-1)^2}{2a^{k+1}}.
\tag{20}
$$

Since $q > p$, the drift that tends to close the nearest gap prevents insertion of particles even if r is large. Thus, both v and D become exponentially small for large k. If $p > q$, the drift tends to open gaps. However, since very large gaps need to be opened to allow insertion of a large k-site particle, the mean velocity and dispersion approach those of a freely diffusing particle: $v = p - q$, $2D = p + q$.

Annealing and zone refinement

Finally, we consider the lattice coverage far from the wall, in the long time limit. The number of particles adsorbed per unit length of translocation may be relevant for considerations about energetics and macromolecular cost. Monomers will cover the translocating polymer behind the wall entirely. Since deposition has been assumed irreversible, the deposition of each particle is associated with a large energy cost, regardless of size. In this case, monomer deposition may be more costly than deposition of larger particles, for which the same energy
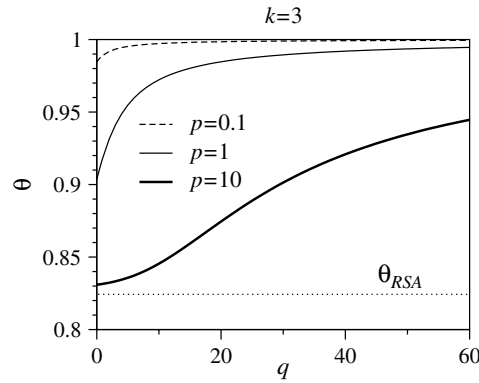
Figure 4. Particle coverage θ behind the wall as a function of q for $k = 3, r = 1$ and various p. For walls that move forward rapidly, $p \to \infty$, the coverage corresponds to that of irreversible RSA on an infinite lattice without a wall and $\theta_{RSA}(k = 3) = 3\sqrt{\pi}e^{-4}(\text{Erfi}(2) - \text{Erfi}(1))/2 = 0.823\,653$ (dotted line). For $p \to 0$, the wall slowly sweeps across the lattice, allowing more contiguous deposition behind it. In this case, $\theta(k, p \to 0) \sim 1$.

loss leads to a larger coverage. Particles of length $k > 1$ also allow the presence of empty gaps at saturation, further minimizing the number of deposited particles.

To quantify a particle cost associated with translocation, consider the infinite-time coverage $\theta \leqslant 1$ representing the fraction of filled lattice sites far behind the moving wall. For monomers, every site will eventually be filled and $\theta(k = 1) = 1$. For $k > 1$, we compute $\theta(k)$ by considering the deposition of a particle into the first gap nearest the wall, splitting it into two. One of these daughter gaps becomes the new 'first' gap closest to the wall, while the other one is now an 'interior' gap. Particles will continue to deposit into the interior gaps, following rules of deposition into a finite length segment [22, 23], until these gaps reach a fixed coverage. For long times, we can calculate the total coverage by summing the saturated coverage of all the interior gaps. For one particular realization of the random sequential ratchet, the creation rate of interior gaps of length m from a first gap of length m' by particle deposition obeys $\dot{N}_m(t) = r H_{m'-m-k}$, where N_m is the number of interior gaps of length m. The Heaviside function prevents the creation of a new interior gap if the original first gap is not long enough to accommodate the particle and the new gap. Ensemble averaging leads to $\langle \dot{N}_m \rangle = r R_{m+k}$, where R_{m+k} is the probability for the first gap to be larger than $m + k$ and $\langle N_m \rangle$ is the ensemble average. At long times, R_{m+k} reaches steady state and the generation of interior gaps grows linearly in time $\langle N_m(t) \rangle \simeq rt R_{m+k}$.

Interior gaps created by this process are themselves filled by further particle deposition. At saturation, an interior gap of initial length m reaches coverage θ_m, a quantity that can be calculated by standard RSA techniques [22, 23]. Each interior gap is bound on each end by a particle of length k. The total initial length of one of these interior gaps and an associated end particle is $m + k$. After further particle deposition into this gap, the number of covered sites reaches $m\theta_m + k$. On weighting over the ensemble-averaged gap length distribution $\langle N_m \rangle$, the coverage can thus be expressed as

$$\theta = \frac{\sum_{m=0}^{\infty}(m\theta_m + k)R_{m+k}}{\sum_{m=0}^{\infty}(m + k)R_{m+k}}. \tag{21}$$

Summary and conclusions

In figure 4, we plot $\theta(k = 3)$ as a function of q, for $p = 0.1, 1, 10$. For small q and large p, the wall moves forward rapidly, largely independent of deposition. The depositing particles rarely interact with the wall and the coverage approaches that of standard RSA on an infinite lattice, θ_{RSA} [15]. If q is large and p is small, the wall stays close to the nearest particle, occasionally leaving gaps only slightly larger than k in which particles can deposit. Thus, the wall slowly sweeps through the lattice, 'zone-refining' it by slowing down the deposition process and allowing for more complete filling. For intermediate values of p, q, we find that the coverage left by the wall is always between the contiguous and RSA limits.

In summary, we have found an exact steady-state velocity of the discrete translocation problem in the limit of irreversible particle attachment. The exact gap distribution R_m given by equations (9)–(11) allows us to construct the mean velocity from $R_1 \equiv \langle \sigma \rangle$ and equation (4). Smaller particles yield faster translocation and smaller dispersion, while larger particles leave less of the remaining lattice covered. In the protein translocation problem, neglecting the dissociation rate as we have done throughout this study, is a good approximation provided chaperone concentrations >nM. In this limit, the result of Elston [3] approaches our velocity given in equation (19). We also find that the coupling of particle deposition to wall dynamics allows the wall to 'zone-refine' the lattice, producing long time particle coverages $\theta_{\text{RSA}} \leqslant \theta \leqslant 1$.

Our results can be used to guide experimental systems that probe the mechanisms of chaperone-assisted translocation. For example, a comparison of the mean translocation speed v with our exact solution and the dispersion D with our Monte Carlo results, lead to independent values for p and $q R_1$ defined in this paper. By measuring v and D for different driving force $F \propto \ln q$ (by tuning, e.g., a transmembrane potential), one can numerically determine both the particle size k and the effective adsorption rate r. If particle detachments occurring at rate r_d are also considered, a sufficient condition for our solution to the mean velocity v to be accurate is $r_d \ll v\theta_{\text{RSA}}/k$. For larger detachment rates, we expect a stall force, where the mean velocity vanishes, and may be negative for large enough F. In this case, the ratcheting occurs with pawls that detach, allowing occasional backsliding to the second particle.

Acknowledgments

References

[1] Simon S M, Peskin C S and Oster G F 1992 What drives the translocation of proteins? *Proc. Natl Acad. Sci.* **89** 3770
[2] Peskin C S, Odell G M and Oster G F 1993 Cellular motions and thermal fluctuations: the Brownian ratchet *Biophys. J.* **65** 316
[3] Elston T C 2002 The Brownain ratchet and power stroke models for posttranslational protein translocation into the endoplasmic reticulum *Biophys. J.* **82** 1239
[4] Gerland U, Bundschuch R and Hwa T 2004 Translocation of structured polynucleotides through nanopores *Phys. Biol.* **1** 19
[5] Meller A, Nivon L and Branton D 2001 Voltage-driven DNA translocations through a nanopore *Phys. Rev. Lett.* **86** 3435

[6] Turner S W, Cabodi M and Craighead H G 2002 Confinement-induced entropic recoil of single DNA molecules in a nanofluidic structure *Phys. Rev. Lett.* **88** 128103

[7] Zandi R, Reguera D, Rudnick J and Gelbart W M 2003 What drives the translocation of stiff chains? *Proc. Natl Acad. Sci.* **100** 8649

[8] Vale R D and Milligan R A 2000 The way things move: looking under the hood of molecular motor proteins *Science* **288** 88

[9] Simon M and Blobel G 1991 A protein-conducting channel in the endoplasmic reticulum *Cell* **65** 371–80

[10] Schneider H J, Berthold J, Bauer M, Dietmeier K, Guiard B, Brunner M and Neupert W 1994 Mitochondrial Hsp70/MIM44 complex facilitates protein import *Nature* **371** 768

[11] Glick B 1995 Can Hsp-70 proteins act as force-generating motors? *Cell* **80** 11

[12] Kolomeisky A and Phillips H 2005 Dynamic properties of motor proteins with two subunits *J. Phys.: Condens. Matter* **17** S3887

[13] Ambjörnsson T, Lomholt M A and Metzler R 2005 Directed motion emerging from two coupled random processes: translocation of a chain through a membrane nanopore driven by binding proteins *J. Phys.: Condens. Matt.* **17** 3945

[14] Evans J W 1993 Random and cooperative sequential adsorption *Rev. Mod. Phys.* **65** 1281

[15] Bartelt M C and Privman V 1991 Kinetics of irrversible monolayer and multilayer adsorption *Int. J. Mod. Phys.* B **5** 2883

[16] Jeffreys H 1972 *Methods of Mathematical Physics* 3rd edn (Cambridge: Cambridge University Press)

[17] Mai J, Sokolov I M and Blumen A 2001 Directed particle diffusion under 'burnt bridges' conditions *Phys. Rev. E* **64** 011102

[18] Saffarian S, Qian H, Collier I, Elson E and Goldberg G 2006 Powering a burnt bridges Brownian ratchet: A model for an extracellular motor driven by proteolysis of collagen *Phys. Rev. E* **73** 041909

[19] Antal T and Krapivsky P L 2005 'Burnt bridge' mechanism of molecular motion *Phys. Rev. E* **72** 046104

[20] Morozov A Yu, Pronina E, Kolomeisky A B and Artyomov M N 2006 Solutions of burnt-bridge models for molecular motor transport *Phys. Rev. E* **75** 031910

[21] Derrida B 1983 Velocity and diffusion constant of a periodic one-dimensional hopping model *J. Stat. Phys.* **31** 433

[22] Boucher E A 1972 Reaction kinetics of polymer substituents. Neighbouring-substituent effects in pairing reactions *J. Chem. Soc. Faraday Trans.* II **72** 2281

[23] D'Orsogna M R and Chou T 2005 Gaps on irreversible and equilibrated one-dimensional lattices *J. Phys. A: Math. Gen.* **38** 531–42

[24] Watson G N 1952 *Treatise of the Theory of Bessel Functions* 2nd edn (Cambridge: Cambridge University Press)